Quaternary Geochronology 41 (2017) 70–82

Contents lists available at ScienceDirect

Quaternary Geochronology

journal homepage: www.elsevier.com/locate/quageo

Research paper

Variations in luminescence properties of quartz and feldspar from modern fluvial sediments in three rivers

Luke A. Gliganic [a, *], Tim J. Cohen [b], Michael Meyer [a], Ariana Molenaar [a]

[a] Institute for Geology, University of Innsbruck, 6020, Austria
[b] ARC Centre of Excellence for Australian Biodiversity and Heritage, GeoQuest Research Centre, University of Wollongong, 2500, Australia

ARTICLE INFO

Article history:
Received 13 January 2017
Received in revised form
23 June 2017
Accepted 24 June 2017
Available online 27 June 2017

Keywords:
Single-grain
Feldspar
OSL
Post IR-IRSL
Fluvial

ABSTRACT

Studies of modern sediments, their sedimentology and depositional processes are important for understanding the behaviour of the luminescence characteristics of quartz and feldspar in fluvial settings. Previous studies have shown large variations in OSL characteristics of quartz from different fluvial systems, while the IRSL and pIRIR signals from K-feldspar have been understudied. We test the effects of fluvial setting on luminescence characteristics by collecting modern (<1 year old) bedload sediments down the courses of three river systems with very different hydrological characteristics, geologic contexts, and catchment lithologies. The single grain (SG) and multi-grain aliquot (MGA) OSL (quartz) and IRSL and pIRIR (K-feldspar) properties of samples were measured and compared to better understand intra- and inter-fluvial system patterns in sensitivity, bleaching, and equivalent dose (D_e) distribution skewness and kurtosis. The quartz OSL and K-feldspar IRSL and pIRIR signal sensitivities increase with downstream transport distance of sediments, confirming previous studies (quartz) and showing that IRSL signals from K-feldspar also increase in response to reworking cycles. Increasing transport distance also results in better bleaching of the OSL signal from quartz samples (MGA and SG) due to more grains being exposed to sunlight. By contrast, the IRSL and pIRIR signals retain significant residuals in all samples, though 5–15% of grains yield zero-dose D_e values and age modelling of SG data yields accurate burial dose estimates. Additionally, the skewness and kurtosis of SG OSL D_e datasets from one river increase with transport distance, with the best bleached samples exhibiting the highest skewness, thereby questioning the applicability of the skewness-value of a D_e dataset as an accurate indicator for partial-bleaching. Our data shows marked variability between (i) different river systems and (ii) the measured minerals, however consistent use of statistical models allows accurate D_e estimation in all contexts. Age modelling of SG data from K-feldspar, thus, provides a valuable tool for future fluvial research in regions where poor OSL characteristics prevent the use of quartz as a dosimeter.

1. Introduction

Constraining the timing and nature of fluvial aggradation and erosion via optically stimulated luminescence (OSL) and infrared (IR) stimulated luminescence (IRSL) dating techniques enables sedimentologists and Quaternary scientists to tackle tectonic, climatic, and palaeohydrologic questions (Mukul et al., 2007; Thomas et al., 2007; Sawakuchi et al., 2012; Jansen et al., 2013). However, sediments that were transported and deposited by fluvial processes present a suite of problems that complicate the estimation of accurate luminescence burial ages. Since optical-luminescence dating methods are used to provide an estimate of the time elapsed since luminescent minerals (quartz – OSL; K-feldsapr – IRSL) were last exposed to sunlight, a major assumption of this method is that the grains are exposed to sufficient sunlight to bleach their latent luminescence signal (Huntley et al., 1985; Rhodes, 2011). In fluvial settings, incomplete resetting of the latent luminescence signal, due to attenuation of sunlight through a sediment-laden water column and short transport distances during low-light conditions, can be problematic and result in age overestimations (Murray et al., 1995; Olley et al., 1999; Stokes et al., 2001).

One approach for understanding these problems is to investigate the residual luminescence signal in aliquots (single- or multi-

* Corresponding author.
E-mail address: luke.gliganic@uibk.ac.at (L.A. Gliganic).

http://dx.doi.org/10.1016/j.quageo.2017.06.005
1871-1014/

grain) of sediments from modern floodplains or active channels (Murray et al., 1995; Olley et al., 1999; Stokes et al., 2001; Jain et al., 2004; Singarayer et al., 2005; Fiebig and Preusser, 2007; Alexanderson, 2007; Hu et al., 2010; Alexanderson and Murray, 2012; McGuire and Rhodes, 2015). Two general, though not ubiquitous, observations are evident. Firstly, modern fluvial sediments usually contain some quartz grains that yield near-zero equivalent dose (D_e) values that would be unlikely to result in significant age overestimations for older sediments (e.g., sediments older than 1 ka according to Jain et al., 2004), while K-feldspar grains yield variable results; some studies report small IRSL residuals (McGuire and Rhodes, 2015) and others report significant IRSL and/or pIRIR residuals (Trauerstein et al., 2014; pIRIR in McGuire and Rhodes, 2015). Secondly, bleaching often improves with transport distance, as indicated by decreasing residual D_e values with distance downstream (Stokes et al., 2001; MET-pIRIR signal in McGuire and Rhodes, 2015), though this is not always observed (e.g., Hu et al., 2010; IRSL signal in McGuire and Rhodes, 2015).

A second approach used to investigate, identify and overcome partial bleaching is to measure many individual grains. This approach allows those fully bleached grains to be identified in a population that includes incompletely bleached grains, which will yield overestimates of the true burial age when combined on the same multi-grain aliquot (MGA) (Arnold and Roberts, 2009; Nian et al., 2012). Many researchers have suggested that the combination of completely and incompletely bleached grains will yield positively skewed single grain (SG) D_e distributions (Olley et al., 1999; Bailey and Arnold, 2006; Summa-Nelson and Rittenour, 2012). Statistical models are subsequently used to isolate the grains that were sufficiently bleached (Olley et al., 1998; Galbraith et al., 1999; Lepper et al., 2000; Thomsen et al., 2007), with the assumption that calculating weighted mean D_e values (e.g., with the central age model) will result in similar overestimates as measuring MGAs.

The problems of partial bleaching are magnified when using the IRSL or pIRIR signal from K-feldspar grains, which are less bleachable than the OSL signal from quartz (Godfrey-Smith et al., 1988; Lawson et al., 2012; Colarossi et al., 2015). Because of this and the near ubiquity of anomalous fading of the IRSL signal in K-feldspars (Spooner, 1994; Huntley and Lamothe, 2001), the quartz-OSL signal from fluvial sediments has been the preferred luminescence dosimeter and received more thorough investigation. However, many regions and geomorphic contexts (e.g., alpine and tectonically active settings) lack sensitive quartz grains but have quite sensitive K-feldspar grains (Preusser et al., 2006; Fuchs et al., 2013; Rhodes, 2015). Recent advances have identified low- or non-fading signals (e.g., pIRIR signals – Thomsen et al., 2008), which are unfortunately more difficult to bleach (Lowick et al., 2012). This necessitates the use of K-feldspar to address research questions and, thus, a better understanding of the behaviour of the IRSL and pIRIR signals of fluvially transported K-feldspar grains is needed to ensure the use of optimal measurement and data analysis procedures to obtain accurate burial ages (Rhodes, 2015).

This study aims to address three specific questions. Firstly, how do OSL/IRSL/pIRIR characteristics (e.g., residual De/bleaching, luminescence sensitivity, SG D_e distribution skewness and kurtosis) change with transport distance in a given fluvial system? Secondly, do different fluvial systems with varying hydrologic characteristics yield different luminescence characteristics? Thirdly, what measurement and data analysis procedures yield the most robust IRSL and pIRIR ages? These aims were approached by collecting modern (<1 year old) bedload sediments along three river systems with very different hydrological characteristics, geologic contexts, and catchment lithologies: Cooper Creek (arid central Australia), Wollombi Brook (temperate eastern Australia), and the Pitze River (European eastern Alps). The chosen rivers represent end-members of a litho-luminescence spectrum; the Australian rivers carry bedload that is quartz rich with well-behaved OSL signals and no K-feldspars while the alpine Pitze River transports insensitive quartz and K-feldspar with bright IRSL and pIRIR signals. The SG and MGA OSL (quartz) and the SG and MGA IRSL and pIRIR (K-feldspar) properties of samples were measured and compared to better understand intra- and inter-fluvial system patterns in sensitivity, bleaching, and D_e distribution skewness and kurtosis. The variability in the observed patterns is discussed along with possible explanations and implications.

2. Experimental procedures and sampling sites

To address the aims of this study 17 samples were collected from fluvial bedforms (channel bars) that were less than one year old at the time of sampling at different locations down the long profile of three different rivers (Fig. 1). The mode of deposition is known and only samples with clearly observable bedding features were used in this study, thus guaranteeing that post-depositional mixing could not have affected the D_e distributions. Likewise, since the age of each deposit is known to be very young, any spatial heterogeneity in the dose rate of the current depositional setting will not have had time to affect D_e distributions, although unbleached grains may retain the inherited effects of heterogeneous dose rates of their previous depositional setting. Consequently, any grains that yield non-zero D_e values must have been incompletely bleached during the last episode of fluvial transport; their residual doses could reflect (i) unbleached dose remaining after exhumation from bedrock or (ii) a burial dose acquired during storage in the floodplain before the most recent fluvial transport event. Two of the rivers (Cooper Creek and Wollombi Brook) are in Australia and have no K-feldspar, but do have quartz with a bright OSL signal that is dominated by the fast component (Table 1). The third river (the Pitze River) is located in the Austrian Alps and drains a catchment with insensitive quartz but bright K-feldspar with minimal fading (see discussion below and Table 2). Single grains of quartz (Australian rivers) and K-feldspar (Pitze River) were measured in addition to large multi-grain aliquots.

Cooper Creek and Wollombi Brook are both ephemeral rivers that have very different hydrographic characteristics, catchment sizes, and lengths (Figs. 1 and 2). Cooper Creek is an order of magnitude longer than Wollombi Brook, has a catchment area that is two orders of magnitude larger (>300,000 km^2 vs 1,848 km^2) and has a flow hydrograph period that is an order of magnitude longer (weeks vs hours). Cooper Creek is a low gradient (200 mm/km) multi-channel river system flowing from the seasonally wet tropics and sub-tropics into the arid interior of the Australian continent. It passes through synclinal basins which store sediment in subsiding 50 km wide floodplains for 10^5–10^6 years (Nanson et al., 2008; Jansen et al., 2013) and through linear dunefields of Australia's central desert. A long history of Late Palaeocene–Early Eocene basin sedimentation through to the present characterises the sedimentary setting with various sediment sinks, provenances and interactions of fluvial, aeolian, and lacustrine processes (Habeck-Fardy and Nanson, 2014). Hydrographs on the Cooper Creek are extended and often last for months (Fig. 2a). By contrast, Wollombi Brook is a river channel <100 km in length in a confined valley (often < 1 km wide) that cuts through a catchment dominated by a single lithology (Triassic sandstones; Rasmus et al., 1969) with sedimentation limited to small Holocene terraces (Erskine and Melville, 2008). There are no significant sediment sinks, and once exhumed from bedrock, grains will be transported down the length of the river during the infrequent flow events. Peak discharges in this sand bed system are rainfall-driven and tend to last for <12 h

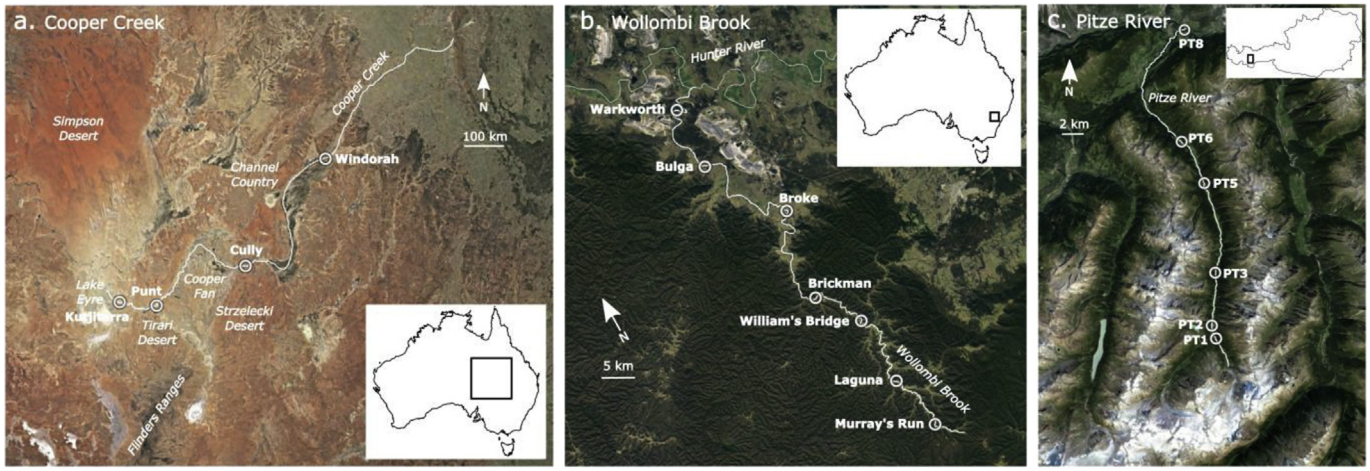

Fig. 1. Sample locations and pertinent landscape features for the (a) Cooper Creek, Australia, (b) Wollombi Brook, Australia, and (c) Pitze River, Austria. Location of each figure is shown as an inset to each figure.

Table 1
Sample data and dose recovery (MGA and SG) data for quartz samples from the Cooper Creek and Wollombi Brook.

River	Sample name	Sample location	Distance downstream (km)	Fast ratio	n=	MGA Measured/Given ratio	n = SG accepted	SG Measured/Given ratio
Cooper Creek								
	CC1	Windorah	600	25.7	6	1.02 ± 0.01	37	1.04 ± 0.02
	CC2	Cullyamurra	1047	26.5	6	1.00 ± 0.01		
	CC3	Punt-Crossing	1433	25.8	6	0.95 ± 0.01		
	CC4	Kutjitara	1552	30.2	7	0.98 ± 0.01	48	0.98 ± 0.02
Wollombi Brook								
	WB1	Murray's Run	11	40.7	7	1.05 ± 0.01	42	1.03 ± 0.02
	WB2	Laguna	22	30.5	7	1.04 ± 0.01		
	WB3	William's Bridge	39	23.6	6	1.03 ± 0.01		
	WB4	Brickman	50	24.3	6	1.05 ± 0.01		
	WB5	Broke	70	28.9	7	1.04 ± 0.01		
	WB6	Bulga	90	29.2	6	1.03 ± 0.01		
	WB7	Warkworth	103	33.5	6	1.02 ± 0.01	61	1.05 ± 0.01

Table 2
Sample data, dose recovery data, and fading data for the IRSL and pIRIR signals from K-feldspar samples from the Pitze River.

Sample name	Distance downstream (km)	Signal	MGA data				SG data			
			n=	Measured/Given ratio	n=	Residual (Gy)	g-value (%/decade)	n = SG accepted	Measured/Given ratio	Over-dispersion	g-value (%/decade)
PT1	4	IRSL	4	0.99 ± 0.02	4	1.95 ± 0.05	2.6 ± 0.2	153	1.01 ± 0.02	15 ± 2	1.04 ± 0.13
		pIRIR	4	1.28 ± 0.02	4	4.26 ± 0.08	0.6 ± 0.2	120	1.27 ± 0.03	20 ± 2	0.65 ± 0.25
PT2	5	IRSL	4	1.00 ± 0.02	4	2.08 ± 0.05					
		pIRIR	4	1.24 ± 0.02	4	4.09 ± 0.08					
PT3	11	IRSL	4	1.21 ± 0.02	4	2.90 ± 0.05	3.6 ± 0.2				
		pIRIR	4	1.31 ± 0.02	4	4.12 ± 0.06	0.4 ± 0.2				
PT5	20	IRSL	4	1.25 ± 0.02	4	3.25 ± 0.05		150	1.08 ± 0.02	23 ± 2	0.88 ± 0.12
		pIRIR	4	1.46 ± 0.02	4	6.50 ± 0.10		124	1.13 ± 0.06	49 ± 4	0.32 ± 0.23
PT6	25	IRSL	4	1.15 ± 0.02	4	2.35 ± 0.05					
		pIRIR	4	1.30 ± 0.02	4	4.44 ± 0.06					
PT8	40	IRSL	4	1.11 ± 0.02	4	2.80 ± 0.05	2.2 ± 0.2				
		pIRIR	4	1.58 ± 0.02	4	6.77 ± 0.10	0.8 ± 0.2				

(Fig. 2c). The Pitze River (~40 km long) is a melt water river with its main discharge occurring during summer when snow and glacier melt reach their peaks, and low winter discharge (Fig. 2e). It drains a catchment with a few and relatively steep tributaries. The lithology in the Pitze catchment is mainly composed of para- and orthogneisses that belong to the Ötztal-Stubai Complex (i.e. crystalline basement rocks of the Eastern Alps). The unit underwent several phases of metamorphism, but most pronounced in the Pitztal area is the Variscan metamorphic event reaching amphibolite facies that was later overprinted by the Eo-alpine and the alpine metamorphic events (Mogessie et al., 1985; Pfiffner, 2009). The valley floor is narrow (<0.5 km wide) with Holocene terraces and alluvial and debris fans that are sourced from the steep (≤35°) valley slopes and are partly active.

3. Methods – equivalent dose determination and evaluation

This study is restricted to fluvial bedforms that were sampled

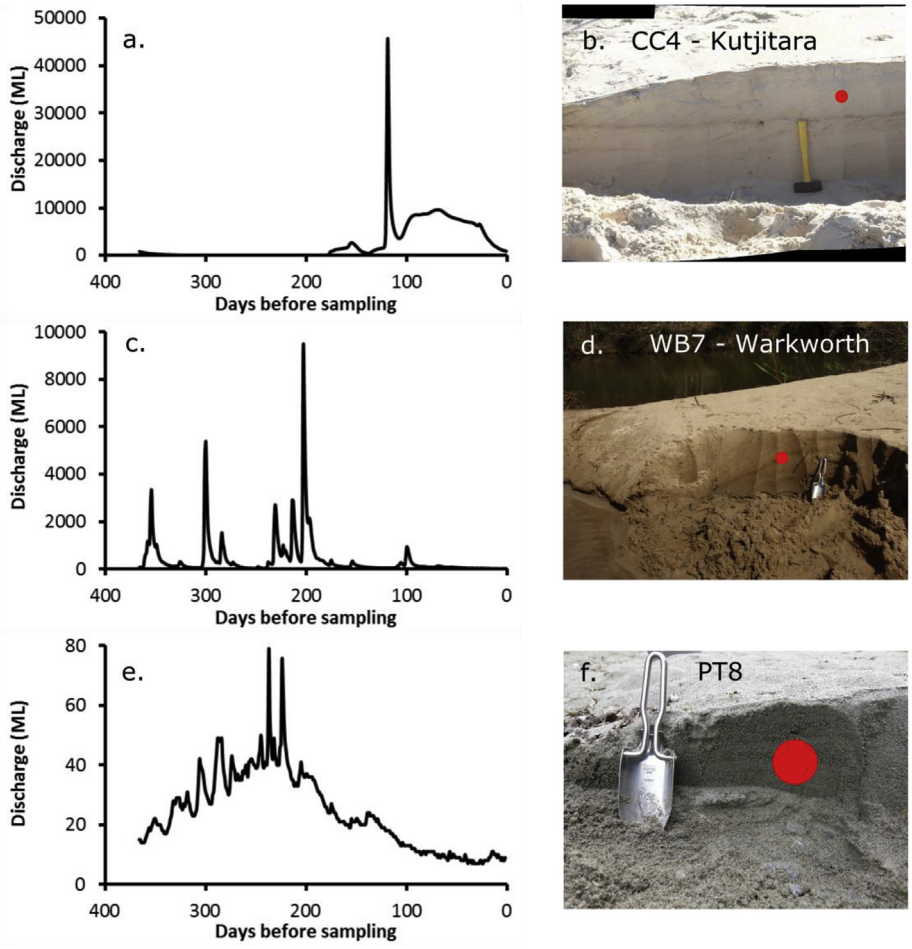

Fig. 2. Flow data for the year before sampling and photos of sampled bedforms with sample locations (red circles, which represent 5 cm-diameter sampling tube) from our study areas. a) Cooper Creek flow data from Cullyamurra (01/07/2011–30/06/2012: www.waterconnect.sa.gov.au) and (b) a photo of CC4 from Kutjitara. c) Wollombi Brook flow data from Brickman (22/09/2011–21/09/2012: www.waterinfo.nsw.gov.au) and (d) a photo of WB7 from Warkworth. e) Pitze River flow data from St. Leonhard im Pitztal (24/03/2014–23/03/2015: http://ehyd.gv.at/) and (f) a photo of PT8. (For interpretation of the references to colour in this figure legend, the reader is referred to the web version of this article.)

not more than a year after deposition. Only unvegetated bars that had original undisturbed surface features (e.g., ripples) and were within one vertical meter of the water level at the time of sampling were investigated. Likewise, sampling was completed during periods of low flow that were preceded by periods of much higher peak discharge (see Fig. 2), thus ensuring that all bars were actively deposited within the last year. Fluvial bars in the modern channels were trenched and photographed (Fig. 2b,d,f). Samples for OSL investigations were collected from each bar by pushing a 5 cm-diameter opaque PVC tube into cleaned sections. Samples were collected from between 5 and 15 cm depth-below-the surface of the bar in the uppermost foreset beds (Fig. 2). Bars without clear bedding features were not used to guarantee that the investigated sand grains have not experienced any mixing since transport and deposition. No dose rate measurements were made since (i) this study is focusing on the effect of downstream transport on D_e distributions and (ii) the age of each bar is known to be < 1 year old.

Quartz and K-feldspar grains of 180–212 μm diameter were extracted from the sediment samples in the laboratory under dim red illumination using standard procedures (Wintle, 1997). Hydrochloric acid (32%) and hydrogen peroxide (50%) were used to remove carbonates and organics, respectively. A sodium polytungstate (SPT) solution with a density of 2.70 g/cm3 was used to isolate quartz and feldspar grains from heavy minerals. A SPT solution of 2.62 g/cm3 was then used to separate feldspars from quartz fractions. Two final SPT solutions of 2.58 and 2.52 g/cm3 were used to isolate K-feldspar grains. Quartz and feldspar grains were soaked in hydrofluoric (HF) acid (40% for 40 min for quartz and 10% for 40 min for feldspars) to remove the external, alpha-dosed layer and any eventually remaining feldspar contamination on quartz separates (Aitken, 1998). Finally, grains were rinsed in hydrochloric acid and sieved again to retain the 180–212 μm diameter fraction. Grains were loaded into a Risø TL/OSL reader and were optically stimulated by blue LEDs (470 ± 30 nm), IR LEDs (875 nm), a green laser (532 nm), or an IR laser (150 mW 830 nm) (Bøtter-Jensen et al., 2003), and photons were measured using an Electron Tubes Ltd 9635Q photomultiplier tube. The ultraviolet OSL emissions from quartz were measured through 7.5 mm of Hoya U-340 filter, while the IRSL emissions from K-feldspars were measured through a Schott BG39 and Corning 7–59 filter set. Optical stimulations of multi-grain aliquots of quartz were performed for 40 s (at 90% power) at 125 °C and D_e values were estimated by summing the first 0.8 s of signal and using the final 8.16 s as background. Single quartz grains were stimulated for 2 s (at 90% laser power) at 125 °C and equivalent doses were estimated by summing the first 0.17 s of signal and using the final 0.3 s as background. Multi-grain aliquot pIRIR measurements (Thomsen et al., 2008) of K-feldspar were performed by stimulating aliquots with the IR LEDs for 100 s at 50 °C, followed by a second stimulation with the IR LEDs for 100 s at 225 °C and equivalent doses were

estimated for both the IR (50 °C) and pIRIR (225 °C) signals by summing the first 2 s of signal and using the final 20 s as background. Single K-feldspar grains were stimulated for 2 s (at 90% laser power) at 50 °C and then stimulated for 2 s (at 90% laser power) at 225 °C, and D_e values were estimated by summing the first 0.17 s of signal and using the final 0.3 s as background. For all K-feldspar measurements, D_e values were calculated using both the IRSL (50 °C) bleach and the pIRIR (225 °C) signals; these signals are referred to as 'IRSL' and 'pIRIR' in the text. Laboratory irradiations were given using calibrated $^{90}Sr/^{90}Y$ beta sources mounted on Risø TL/OSL readers.

For each quartz sample, 24 aliquots composed of ~400 grains (5 mm mask) and 500 single grains were measured using the single-aliquot regenerative-dose (SAR) procedure (Murray and Wintle, 2000). Preheats of 180 °C for 10 s and 160 °C for 5 s were applied prior to the optical measurement of the natural/regenerative dose and test dose, respectively. Standard tests were applied to ensure the appropriateness of the SAR procedure. These include dose recovery experiments (Murray and Wintle, 2003; 1000 s blue LED bleach for MGA and 1 h solar simulator bleach for SG), a zero-regenerative dose check for recuperation, a repeat-regenerative dose for calculation of a recycling ratio to ensure that sensitivity changes are being corrected for (recycling ratio within 2σ of unity) (Murray and Wintle, 2000), and, for SG quartz measurements, an OSL-IR depletion ratio test (Duller, 2003) to identify and eliminate contaminant feldspar grains. For K-feldspar samples, 12 aliquots composed of ~400 grains (5 mm mask) and 300 single grains were prepared and measured using a pIRIR procedure using a regenerative and test dose preheat of 250 °C for 60 s. Dose recovery and residual-measurement experiments (6 h solar simulator bleach) and fading measurements were also performed for MGAs and single grains from these samples. Laboratory IRSL and pIRIR fading rates were measured for 10–12 multi-grain aliquots of K-feldsapr from each of three samples (PT1, PT3 and PT8) and 200 individual grains from each of two samples (PT1 and PT5). Fading assessments were based on repeated Lx/Tx measurements with delay times between dose/preheat and IRSL/pIRIR measurement between 0.1 h and 223 h (Auclair et al., 2003). Estimates of g-value (percent of signal loss per decade of storage time) were calculated by plotting sensitivity corrected IRSL/pIRIR signals against delay time (Huntley and Lamothe, 2001).

Statistical models used to analyse D_e data were implemented using the Luminescence R package (Kreutzer et al., 2012). The central age model (CAM; Galbraith et al., 1999) and the 3-parameter minimum age model (MAM; Galbraith et al., 1999) were used for MGA data, while the unlogged CAM (ul-CAM; Arnold et al., 2009) and the unlogged 3-parameter MAM (ul-MAM; Arnold et al., 2009) were used to analyse SG data, which often included negative D_e values. The MAM and ul-MAM were both applied with a 10% overdispersion. Additional parameters used to describe D_e distributions include the overdispersion (calculated using the CAM), skewness, kurtosis, and the percentage of zero-dose grains (i.e., grains yielding a D_e consistent with zero). The criteria described by Gliganic et al. (2016) were used in tandem to identify zero-dose grains: (i) grains with D_e values that are consistent with 0 at 2σ and (ii) less than 5 Gy; the latter criterion removes the influence of high-dose D_e values with very low precisions. The sensitivity of the skewness parameter to outlier D_e data was tested by sequentially removing the highest D_e values (i.e., the highest De, the highest two D_e values, and the highest three D_e values).

Luminescence sensitivity was quantified using the average mass-normalised T_n (the OSL, IRSL, or pIRIR signal measured following the application of the test dose following the measurement of the natural and the weight of grains on each disc) from 24 MGAs from each sample. All sensitivity data for a given river were measured using the same Risø TL/OSL reader, with reader dose rates of 0.030 Gy/s (WB and CC samples) and 0.107 Gy/s (PT samples). Where applicable (see Results below), these sensitivity data allow an assessment of the effect of transport distance and repeated cycles of sediment reworking on luminescence brightness (e.g., Pietsch et al., 2008; Sawakuchi et al., 2011). To explore this relationship between repeated reworking cycles and K-feldspar IRSL and pIRIR signal brightness in the laboratory, a similar experiment to that reported by Pietsch et al. (2008 - Table 3) was performed. To begin, K-feldspar aliquots of the most upstream sample (PT1) were given a regenerative dose cycle (preheated, stimulated with IR at 50 °C, then stimulated with IR at 225 °C, followed by a test dose cycle with a test dose of 5 Gy). Next, subsets of four aliquots were exposed to various numbers (0, 10, 20, 100, 200, 500) of simulated reworking cycles, which consisted of cycles of irradiation (5 Gy) and blue LED stimulation (40 s at 50 °C). Finally, a second regenerative dose cycle was performed. The test dose measurements were then compared to each other to assess how sensitivity changed as a function of dosing and optical stimulation cycles. To assess any possible effects of the repeated heating of samples to 50 °C during simulated reworking cycles, the experiment was repeated with fresh aliquots (two aliquots per subset) and the simulated reworking cycles were replaced by repeated cycles of 50 °C anneals (held for 40 s).

4. Results

4.1. Dose recovery and fading results

Dose recovery experiments performed using MGAs and SGs of quartz from samples from Cooper Creek and Wollombi Brook (Table 1) showed several important features of the measured samples. Firstly, the sample average OSL-IR depletion ratios of 1.01 ± 0.04 (Wollombi Brook) and 1.00 ± 0.01 (Cooper Creek) show that the measured quartz extracts are not contaminated by feldspars. Secondly, the OSL signals from all samples yield 'fast ratios' (Durcan and Duller, 2011) between 24 and 41 indicating that they are dominated by the fast component. Thirdly, the satisfactory measured/given dose ratios (Table 1) show that the SAR procedure is suitable for accurately estimating equivalent dose values for the measured samples.

Eight MGAs of K-feldspar grains from each Pitze River sample were bleached and then given a 10 Gy laboratory irradiation (4 MGAs per sample) or given no dose (4 MGAs per sample). Following the dose recovery, MGAs of PT1, PT3 and PT8 were used for fading assessment. The IRSL signal yields a slightly overestimating measured/given dose ratio (1.11 ± 0.01: n = 24), which is corroborated by the measured residual dose (2.55 ± 0.02 Gy: n = 24). The average laboratory fading rate is 2.7 ± 0.3%/decade. The pIRIR signal shows a higher average measured/given dose ratio of 1.35 ± 0.01 (n = 24) and a correspondingly higher average residual signal of 4.65 ± 0.03 Gy (n = 24), but a lower laboratory fading rate (0.6 ± 0.1%/decade). SG dose recovery experiments (20 Gy given dose) and fading measurements were performed for two Pitze samples (PT1 and PT5). Combined SG IRSL results from both samples yield a measured/given dose ratio of 1.05 ± 0.01 (n = 303, overdispersion = 20 ± 1%) and a weighted mean g-value of 0.95 ± 0.09%/decade. The SG pIRIR signal yielded a measured/given dose ratio of 1.20 ± 0.03 (n = 244, overdispersion = 39 ± 2%), and a weighted mean g-value of 0.47 ± 0.17%/decade. The measured SG fading rates are very low (<1%/decade) and would result in grains with low D_e values (~5 Gy) losing only ~7% (IRSL) and ~4% (pIRIR) of their signal during burial.

Table 3
SG quartz OSL data for samples from Cooper Creek and Wollombi Brook.

River	Sample name	Measured/accepted	Skew	Kurtosis	Modern grains (%)	OD (%)	ul-CAM D_e (Gy)	ul-MAM D_e (Gy)
Cooper Creek								
	CC1	500/66	2.4	5.3	42	70 ± 9	2.87 ± 0.57	0.09 ± 0.06
	CC2	500/66	4.1	17.9	89	95 ± 18	0.03 ± 0.03	−0.01 ± 0.03
	CC3	500/32	1.6	5.4	100	0 ± 0	−0.03 ± 0.05	−0.02 ± 0.09
	CC4	500/65	3.4	11.2	75	123 ± 18	0.67 ± 0.19	0.08 ± 0.04
Wollombi Brook								
	WB1	500/98	1.3	1.0	22	49 ± 5	4.43 ± 0.42	0.17 ± 0.10
	WB2	500/65	1.2	3.4	98	0 ± 0	−0.04 ± 0.03	−0.05 ± 0.05
	WB3	500/113	2.0	4.2	50	56 ± 6	2.84 ± 0.37	0.08 ± 0.05
	WB4	500/111	3.5	14.8	76	63 ± 9	0.95 ± 0.19	0.04 ± 0.04
	WB5	500/87	3.7	14.5	90	67 ± 14	0.01 ± 0.03	−0.03 ± 0.03
	WB6	500/100	5.8	36.6	75	100 ± 12	1.13 ± 0.29	0.02 ± 0.03
	WB7	500/104	9.6	94.0	95	63 ± 15	−0.03 ± 0.02	−0.04 ± 0.04

4.2. Cooper Creek

Cooper Creek is the longest river investigated in this study, with samples collected over ~1000 km of the main trunk stream. With only four samples the coverage of this river is inadequate, but is sufficient to make some broad observations. Firstly, SG data (Table 3, Fig. 3a, 3c, S1) show that these fluvial bedload samples contain many well bleached grains. The three downstream samples yield D_e datasets with >75% zero-dose SG D_e values and ul-CAM D_e values between 0 and 0.67 Gy. The most upstream sample is less well bleached, with only 42% of SG D_e values being zero-dose and an ul-CAM value of ~3 Gy. These small residual D_e values are circumvented when the MAM is calculated, as ul-MAM D_e values for all samples are modern in age (consistent with 0 Gy). MGA data shows more variability, with CAM and MAM estimates showing a higher unbleached residual dose, with CAM estimates ranging between ~0.02 Gy and ~6.1 Gy, and MAM estimates ranging between zero-dose and 2.6 Gy. These results indicate that SG measurements can be used to better identify well bleached grains than MGA D_e data. However, the residual dose calculated using the MAM from MGAs is likely too small to yield significant overestimations for samples with burial doses of >30 Gy. Secondly, there appears to be no relationship between luminescence characteristics including bleaching (Fig. 3a and 3c), SG D_e distribution overdispersion (Fig. 3e), skewness or kurtosis (Fig. 3g), or sensitivity (Fig. 4a) with distance downstream; the sensitivity actually appears to decrease with distance downstream (Fig. 4a) which is the opposite of what is expected (e.g., Pietsch et al., 2008). This is likely due to several factors including (i) the complex interactions between sediment sinks and sources and (ii) inadequate sampling along the length of the river (see Section 5.2).

4.3. Wollombi Brook

In contrast to Cooper Creek, Wollombi Brook is an ideal catchment for investigating changes in sediment OSL characteristics downstream. The homogeneous lithology in the catchment and the lack of any major sediment sinks means that sediment begins at the headwaters moves downstream as bedload to the terminus at the confluence with the Hunter River. It is expected that there is additional sediment input down-channel from adjacent bedrock exposures and minor tributaries, but the effects of these sediments should be minor relative to the integrated signal from upstream. In the case of Wollombi Brook, the sensitivity of quartz bedload generally increases with transport downstream (Fig. 4b), though not linearly ($R^2 = 0.22$) or continuously as described by Pietsch et al. (2008).

The D_e distributions of Wollombi Brook samples (Fig. S2) show other changes that correlate with transport distance. With the exception of the sample WB2, the proportion of measured grains that yield zero-dose D_e values (Fig. 3b) continually increases with transport distance, indicating that downstream samples are better bleached. This is reflected in the age model data from this site (Fig. 3d). Two of the most upstream samples yield the lowest proportion of zero-dose SG D_e values and, correspondingly, these samples yield the highest ul-CAM D_e values (between 2.8 and 4.5 Gy). The remaining samples (71%; n = 5) yield SG D_e datasets with 75% or more zero-dose grains and ul-CAM D_e values below 1.15 Gy. Similar to the Cooper data however, the MAM can be used to overcome any residual doses in these data; the ul-MAM yields modern-age D_e values for every sample. The MGA data (Table 4 and inset to Fig. 3d) shows the same general pattern of improved bleaching with transport distance, but CAM and MAM D_e estimates yielding higher unbleached residual doses than SG data. CAM estimates range between ~0.2 Gy and ~5.3 Gy, and MAM estimates ranging between 0.05 Gy and 3.4 Gy. The MGA CAM and MAM estimates are an average of 0.5 Gy and 0.8 Gy, respectively, higher than the SG ul-CAM and ul-MAM estimates. These results indicate that as a grain moves downstream it is more likely to be bleached. Additionally, while bedload samples from Wollombi Brook contain many well bleached grains, residual doses may remain in the SG and MGA data for upstream samples. However, the use of the MAM, particularly on SG data, can overcome these residuals and can be used to determine a D_e value that is representative of the most recent episode of fluvial transport and deposition.

Similar to OSL sensitivity and bleaching, and in contrast to many previous studies (Bailey and Arnold, 2006; Summa-Nelson and Rittenour, 2012) the skewness and kurtosis of the SG D_e datasets increase exponentially (skewness $R^2 = 0.97$ and kurtosis $R^2 = 0.99$) with increasing transport distance (Fig. 3h). The sequential removal of high-De outliers only significantly affects the most downstream sample (WB7) for which only one D_e value is significantly different from the main population. All other samples show the same trend of increasing skewness and kurtosis with transport distance regardless of the removal of the highest D_e values. This increase in skewness and kurtosis of the D_e datasets parallels the increase in the number of well bleached grains (Fig. 3b) and the increasingly accurate CAM (MGA), MAM (MGA), and ul-CAM (SG) age estimates.

4.4. Pitze River

The Pitze River is like Wollombi Brook in that it is a single trunk stream in a narrow valley that drains a lithologically homogeneous catchment and has no significant sediment sinks today. Likewise, the main source of sediment in the Pitze River is glacially eroded bedrock in the headwaters or hillslope landslide material,

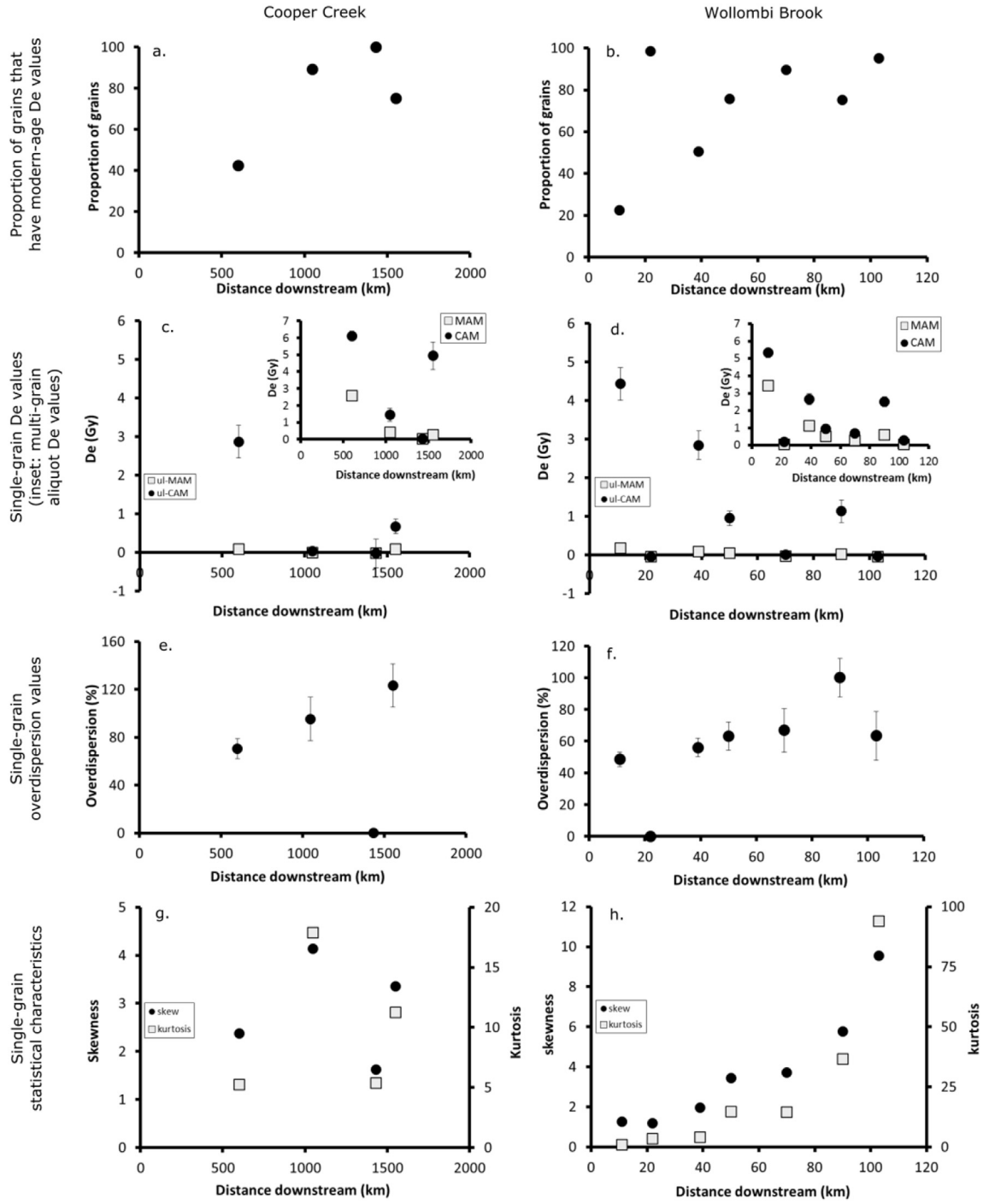

Fig. 3. SG OSL data for quartz samples from Cooper Creek and Wollombi Brook showing (a and b) the proportion of grains that yield modern age D_e values, (c and d), the SG D_e values, (insets to c and d) the multi-grain aliquot D_e values, (e and f), the SG overdispersion values, and (g and h), the skewness and kurtosis of SG D_e distributions.

suggesting that most grains are exhumed in the headwaters and are transported as bedload down river to its terminus at the confluence with the Inn River. Similar to samples from other alpine settings, the quartz extracts from these sediments yield no OSL signal. The K-feldspar extracts, however, yield bright IRSL and pIRIR signals on both the single- and multi-grain level.

Similar to quartz OSL results from Wollombi, the IRSL and pIRIR sensitivities increase with transport distance downstream (Fig. 5a). Interestingly, however, the two signals do not increase in parallel. The pIRIR signal increases linearly with transport distance ($R^2 = 0.97$), mirroring the linear increase in quartz sensitivity reported by Pietsch et al. (2008). By contrast, the IRSL signal increases very steeply over the first three samples, then increases in parallel with the pIRIR signal for three samples, approximating an exponential increase ($R^2 = 0.92$). To explore this observation in the laboratory, repeated reworking cycles were simulated and the IRSL and pIRIR sensitivities measured before and after the repeated irradiation/bleaching cycles were compared (see methods section for experiment description). Results show that the sensitivity of both the IRSL and pIRIR signals increases exponentially (IRSL

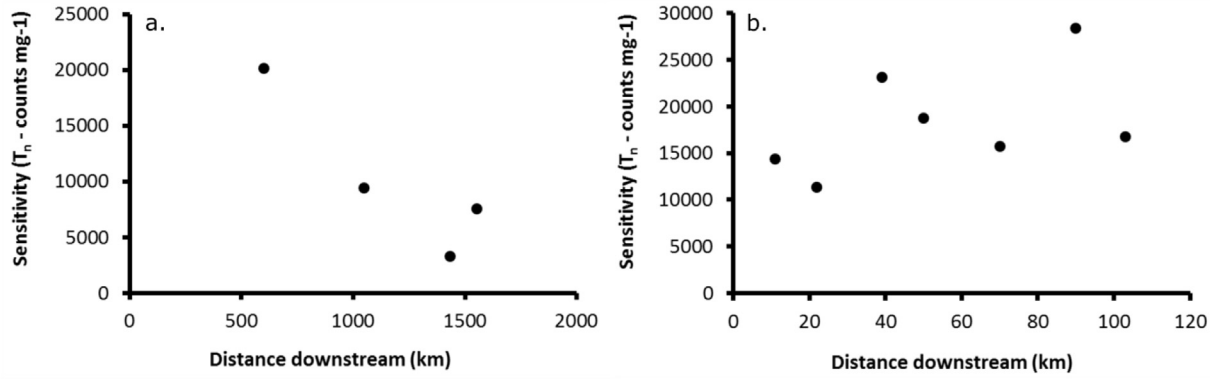

Fig. 4. Quartz OSL sensitivity data from MGA of Cooper Creek (a) and Wollombi Brook (b).

Table 4
MGA OSL data for quartz samples from Cooper Creek and Wollombi Brook.

River	Sample name	n=	Avg T_n[a] (counts)	Kurtosis	Skew	CAM D_e (Gy)	OD (%)	MAM D_e (Gy)
Cooper Creek								
	CC1	24	129,178	9.0	2.6	6.1 ± 0.6	45 ± 6	2.56 ± 0.26
	CC2	24	64,726	9.7	3.0	1.4 ± 0.3	92 ± 13	0.41 ± 0.06
	CC3	24	17,828	2.3	−1.3	0.020 ± 0.004	83 ± 15	0.02 ± 0.01
	CC4	24	54,315	4.3	2.0	4.9 ± 1.1	112 ± 16	0.25 ± 0.04
Wollombi Brook								
	WB1	24	87,667	0.8	0.8	5.3 ± 0.3	30 ± 4	3.42 ± 0.26
	WB2	24	87,643	12.3	3.4	0.2 ± 0.04	85 ± 12	0.06 ± 0.01
	WB3	24	103,489	−0.5	0.6	2.6 ± 0.3	52 ± 8	1.13 ± 0.18
	WB4	24	121,710	9.0	2.6	1.0 ± 0.1	53 ± 8	0.52 ± 0.05
	WB5	24	89,253	7.2	2.5	0.7 ± 0.1	71 ± 10	0.28 ± 0.03
	WB6	24	138,277	7.7	2.9	2.5 ± 0.4	80 ± 12	0.60 ± 0.08
	WB7	24	106,021	11.7	3.0	0.3 ± 0.1	103 ± 15	0.05 ± 0.01

[a] Avg T_n – average of all mass-normalised T_n values from measured samples.

$R^2 = 0.99$ and pIRIR $R^2 = 0.99$), reaching saturation after ~100 cycles at which point a maximum sensitivity is reached (Fig. 6). Repeated heating to 50 °C is shown to have no effect on the IRSL or pIRIR sensitivity (IRSL-control and pIRIR-control in Fig. 6). In contrast to the natural results (Fig. 5a), the IRSL and pIRIR increase in this laboratory experiment at the same rate.

Fig. 5b and Table 5 show MGA IRSL and pIRIR D_e data from Pitze River K-feldspar samples. Both the IRSL and the pIRIR signals contain a very large unbleached residual dose in MGA data (Fig. 5b). The CAM D_e values calculated for IRSL data range between 5.7 Gy and 91 Gy, while the pIRIR CAM D_e values are higher, ranging between 15.6 Gy and 126 Gy. Likewise, the MAM D_e values for IRSL data are between 5.1 Gy and 58.6 Gy, and the pIRIR MAM data range between 13.5 Gy and 80.8 Gy. While the MAM does yield lower dose estimates, they are still significant for all samples and, for most samples, would contribute significantly to overestimating burial doses for most samples.

Fig. 7, Fig. S3, Fig. S4, and Table 6 show the corresponding K-feldspar D_e data on the SG level. In contrast to the MGA data, the SG data yield lower ul-CAM and ul-MAM D_e values for all signals for all samples. The IRSL data yield ul-CAM values between 4 and 35 Gy, while the pIRIR ul-CAM values are between 14 and 45 Gy. Likewise, the ul-MAM D_e values are between 0.2 and 0.8 Gy for the IRSL signal and between modern and 2.6 Gy for the pIRIR signal. The low MAM D_e values are supported by the presence of between 5 and 15% zero-dose grains in each D_e dataset (Fig. 7a and b), indicating that some proportion of grains in each sample was bleached during recent transport.

Finally, in contrast to Wollombi and other published data (e.g., McGuire and Rhodes, 2015) there appears to be no significant pattern in measured D_e values with transport distance. While the most upstream sample yields the lowest MGA CAM and MAM estimates, the remaining samples vary considerably. A possible trend towards higher MGA CAM and SG CAM D_e values further downstream may be seen, but these data are not conclusive. Likewise, and in contrast to data from Wollombi, there is no apparent trend in SG D_e skewness or kurtosis with transport distance, the proportion of zero-dose grains, or CAM D_e value (the latter two criteria representing how well bleached the samples are). In the case of the SG data from the Pitze, skewness and kurtosis measures are not correlated with bleaching.

5. Discussion

5.1. Bleaching of OSL/IRSL signals in bedforms

Each fluvial bedform investigated in this study is known to be < 1 year old and every investigated grain was transported and deposited within the last year, thus allowing us to assess how well bleached each fluvial bedload sample is. For SG quartz data, the proportion of measured grains that yield zero-dose D_e values serves as a proxy for what proportion of grains are completely bleached during, or shortly before transport and deposition. For K-feldspar samples, the presence of anomalous fading of the IRSL and pIRIR signals complicates the direct association between zero-dose D_e values and bleaching. However, low measured SG fading rates (<1%/decade, Table 2) would result in grains with low D_e values losing ~7% (IRSL) and ~4% (pIRIR) of their signal over time. Given the low fading rates of these samples, zero-dose D_e values cannot be produced from unbleached grains with residual IRSL or pIRIR signals. Consequently, the presence of zero-dose D_e values in SG K-feldspar datasets can be interpreted in the same way as those in SG

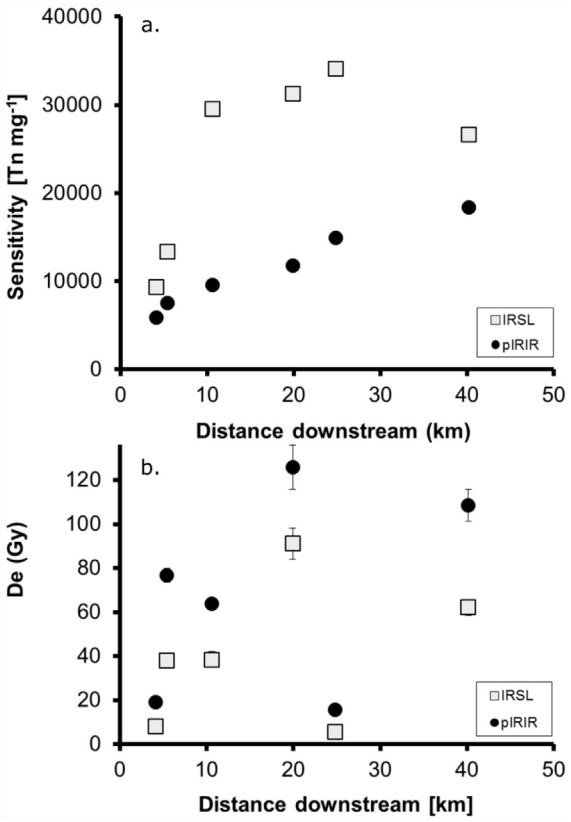

Fig. 5. MGA K-feldspar data for samples from the Pitze River.

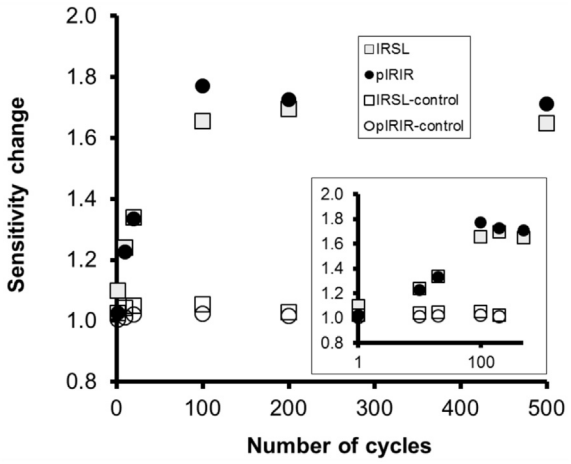

Fig. 6. Results from a laboratory sensitising experiment. MGAs of K-feldspar from PT1 were subjected to repeated simulated reworking cycles of laboratory irradiations and blue LED stimulation (40 s at 50 °C). A control experiment in which aliquots were subjected to repeated cycles of 50 °C anneals is also shown. Inset shows the same data on a log x-axis.

quartz datasets, namely as proxies for grains that were completely bleached during transport.

SG samples from Cooper Creek and Wollombi Brook contain many well bleached quartz grains. Only three samples' SG D_e datasets are comprised of less than 50% zero-dose grains and, correspondingly, these samples yield the highest ul-CAM D_e values (between 2.8 and 4.5 Gy). Meanwhile, the remaining samples ($n = 8$) yield D_e datasets with 75% or more zero-dose grains and ul-CAM D_e values below 1.15 Gy. These results indicate that, even in the worst case, the CAM results from SG data will only overestimate the actual age by ~4.5 Gy. With that in mind, the use of the MAM (or ul-MAM when D_e distributions contain negative D_e values) overcomes any residual values; the ul-MAM yields modern-age D_e values for all samples. These results indicate that incompletely bleached grains are present in SG quartz samples and contribute to a small residual dose, despite the majority of quartz grains being well bleached. However, the use of the MAM can overcome these residuals and be used to determine a D_e value that is representative of the timing of fluvial transport and deposition.

In all quartz samples, MGA data (CAM or MAM) is consistent with, or overestimates SG data. While the largest MGA CAM and MAM residuals are 6.1 ± 0.6 Gy and 3.4 ± 0.3 Gy, respectively, the largest SG ul-CAM and ul-MAM D_e estimates are 4.4 ± 0.4 Gy and 0.2 ± 0.1 Gy, respectively. However, all samples yield accurate SG ul-MAM D_e values that are consistent with zero at 2σ (i.e., modern). These results show that the SG data better approximates the true transport and depositional age, and the use of the MAM on SG data provides the best method for determining the timing of deposition. However, in the case of these quartz bedload samples, while none of the MGA CAM or MAM estimates yield modern-age D_e estimates, CAM and MAM D_e values of less than 1.5 Gy are calculated for 9 samples. This magnitude residual value is usually insignificant when older samples are being investigated but could be significant in low dosing environments for geologically young deposits (e.g. Holocene). These results indicate that, for Cooper Creek and Wollombi Brook quartz samples, SG measurements can be used to identify well bleached grains better than MGA measurements, but the residual doses calculated using the MAM from MGAs is probably not significant for samples with burial doses of >30 Gy. The best practice for estimating accurate burial ages of these fluvial quartz samples is to calculate the MAM of SG D_e data.

By contrast to quartz from Wollombi Brook and Cooper Creek, the MGA K-feldspar data from the Pitze River yields very large residual doses (Fig. 5b, Table 5). No samples yield IRSL and pIRIR CAM or MAM D_e estimates that are modern-age, and the residual MGA MAM D_e estimates are very high (as high as 58 Gy and 80 Gy for the IRSL and pIRIR, respectively). Likewise, all samples yield D_e estimates that are significantly higher than the residual dose remaining after 6 h of solar simulator bleaching (Table 2). The SG data shows why MGA CAM and MAM De values are so high (up to 80 Gy); most grains yield non-zero D_e values, with some saturated and class-3 type grains (i.e., L_n/T_n overlying the dose response curve: Yoshida et al., 2000) being observed. Similar to MGA results, the SG CAM yields significant overestimates for all samples (Fig. 7c and 7d, Table 6). However D_e values that were closer to zero could be calculated using the ul-MAM for SG data for both IRSL to pIRIR. The D_e data show that, while many K-feldspar grains are poorly bleached or have significant residual doses, between 5 and 15% of grains are fully bleached during transport/deposition (Fig. 7a and 7b). For fluvially transported K-feldspar samples from the Pitze River, the residual remaining in MAM estimates derived from MGAs would result in significant overestimating burial doses. By contrast, the use of the MAM for SG D_e data from samples with low fading rates can identify those few grains that were bleached during transport and can, thus, be used to calculate an accurate burial dose.

5.2. Bleaching and transport distance

As discussed earlier, there are no relationships observed between luminescence characteristics, including bleaching (Fig. 3a and 3c), sensitivity (Fig. 4a), and skewness and kurtosis (Fig. 3g), with distance downstream for the Cooper Creek. However, this is readily explained by the diversity of Quaternary sediment stores

Table 5
MGA IRSL and pIRIR data for K-feldspar samples from the Pitze River.

Signal	Sample name	n=	Avg T_n[a] (counts)	OD (%)	CAM D_e (Gy)	MAM D_e (Gy)
IRSL						
	PT1	12	9333	7 ± 2	8.1 ± 0.2	8.1 ± 0.4
	PT2	12	13,377	17 ± 4	38.0 ± 1.9	33.0 ± 2.5
	PT3	12	29,533	33 ± 7	38.4 ± 3.6	24.7 ± 2.7
	PT5	11	31,240	26 ± 6	91.2 ± 7.1	58.6 ± 7.1
	PT6	11	34,065	13 ± 3	5.7 ± 0.2	5.1 ± 0.4
	PT8	12	26,634	19 ± 4	62.1 ± 3.5	48.6 ± 4.2
pIRIR						
	PT1	12	5849	10 ± 2	19.0 ± 0.6	18.7 ± 1.1
	PT2	11	7510	13 ± 3	76.8 ± 3.0	71.2 ± 5.4
	PT3	12	9586	15 ± 3	63.7 ± 2.8	59.7 ± 4.1
	PT5	12	11,796	28 ± 6	125.9 ± 10.1	80.8 ± 8.6
	PT6	12	14,947	25 ± 5	15.6 ± 1.1	13.5 ± 1.1
	PT8	12	18,361	23 ± 5	108.5 ± 7.2	80.0 ± 7.8

[a] Avg T_n – average of all mass-normalised T_n values from measured samples.

and the more complex interactions with the channel and the adjacent dune sediments and older fluvial sequences, along the length of the channel network (Jansen et al., 2013; Habeck-Fardy and Nanson, 2014). Each sample collected from the Cooper system probably has a different main sediment source, most likely one of the older late Quaternary sequences through which the channel flows (Fig. 1). Bedload in the Cooper at Windorah (CC1) has likely travelled in channel from upriver, possibly as far as the headwaters past Longreach. By contrast, downstream of Windorah is the channel-country, a large Quaternary sediment sink (Jansen et al., 2013) that is being filled by sediment from upriver. Bedload sediments from the upper reaches to the north of Windorah are most likely not transported further downstream. Sand for the next two samples at Cullyamurra (CC2) and the Punt Crossing (CC3) likely have their origins from aeolian sediment from the Strzelecki desert and possibly the northern Flinders Ranges. Finally, the bedload at Kutjitara (CC4) may be fluvially transported downstream from the Cooper fan and/or be aeolian sediments from the adjacent Tirari desert dunes. This series of obstacles to sediment transport from headwaters to terminus and the variable sediment inputs means that a bedload sand grain from the headwaters is unlikely to reach the depot centre. Consequently, OSL characteristics from the Cooper Creek samples are not necessarily comparable to each other or with transport distance.

In contrast to the complexity of Cooper Creek, Wollombi Brook's channel is in a confined valley with no sediment sinks and Holocene terraces (Erskine and Melville, 2008). Consequently, most of the sand grains that comprise modern fluvial bedforms were eroded from bedrock with a saturated OSL signal, transported into the channel, and subsequently transported downstream as bedload. Our OSL data from quartz from Wollombi Brook shows that there is a clear increase in bleaching with increased transport distance downstream; the proportion of zero-dose grains in a given sample increases and the ul-CAM (SG) and CAM (MGA) D_e estimates decrease with distance downstream (Fig. 3b, 3d and inset). This observation is in agreement with Stokes et al. (2001), and indicates that as one moves from upstream to downstream, quartz grains that comprise bedforms have experienced more reworking cycles and, thus, have had more opportunities for sunlight exposure since exhumation from bedrock. These bleaching opportunities can be either subaqueously during transport or subaerially on bar surfaces after deposition (e.g., Gray and Mahan, 2015).

The Pitze River presents a different picture. Whereas the quartz-OSL D_e data for the Wollombi Brook and feldspar MET-pIRIR D_e data from other rivers (e.g., the Mojave River – McGuire and Rhodes, 2015) show a decrease in D_e data with distance downstream, the IRSL and pIRIR signals from K-feldspar from the Pitze River exhibit erratic MGA MAM and CAM results and a general increase in SG ul-CAM D_e values. It is assumed that upon erosion from the bedrock the luminescence signal of an exhumed grain is saturated (McGuire and Rhodes, 2015) and, thus, it is counterintuitive that the most upstream sample is better bleached and that more downstream samples with more opportunities for reworking and bleaching yield higher D_e values. This difference, however, can likely be explained by the differences of the fluvial systems in discharge and bedload transport and catchment topography. The Wollombi Brook and Mojave River (McGuire and Rhodes, 2015) are both ephemeral rainwater rivers with short maximal flow periods and, thus, many opportunities for transport, deposition and subaerial bleaching on bar surfaces. By contrast, the Pitze River has a two-state yearly cycle. During the winter discharge is low and occupies only part of the channel, but the rest of the channel is covered in snow. During summer, snowmelt and glacier ablation peaks and low frequency/high magnitude rain event occur, resulting in peak discharge and bedload transport in the Pitze. While large amounts of sediment are transported during this time, the flow becomes increasingly turbid and inhibits bleaching possibilities. Likewise, these same extreme rain events and summer snowmelt can activate smaller catchments down the length of the Pitze River that can contribute sediment via debris fans, thus contributing unbleached, recently eroded sediments to the bedload. The combination of few bleaching opportunities and occasional bedload rejuvenation can explain the incorporation of more high-dose grains in MGAs and SG CAM estimates.

5.3. Sensitivity changes with transport distance

Several studies have shown that quartz grains increase in brightness with the number of reworking cycles and, by proxy, transport distance in fluvial systems (Pietsch et al., 2008; Sawakuchi et al., 2011). Quartz grains from Wollombi Brook show this expected increase in sensitivity with transport distance, corroborating the results of prior studies. Interestingly, both the IRSL and pIRIR signals from K-feldspar grains also increase with transport distance. Similarly, laboratory experiments show that both the IRSL and pIRIR signals increase with the number of cycles of irradiation and blue LED bleaching (laboratory simulations for burial and transport/sunlight stimulation). However, the laboratory and natural signals increase quite differently. The IRSL and pIRIR signals increase correspondingly during laboratory irradiation and optical stimulation cycles (Fig. 6), with both signals showing an approximately exponential increase until ~100 cycles before no more change is observed. By contrast, the natural IRSL signal increases dramatically in the first three cycles before increasing more

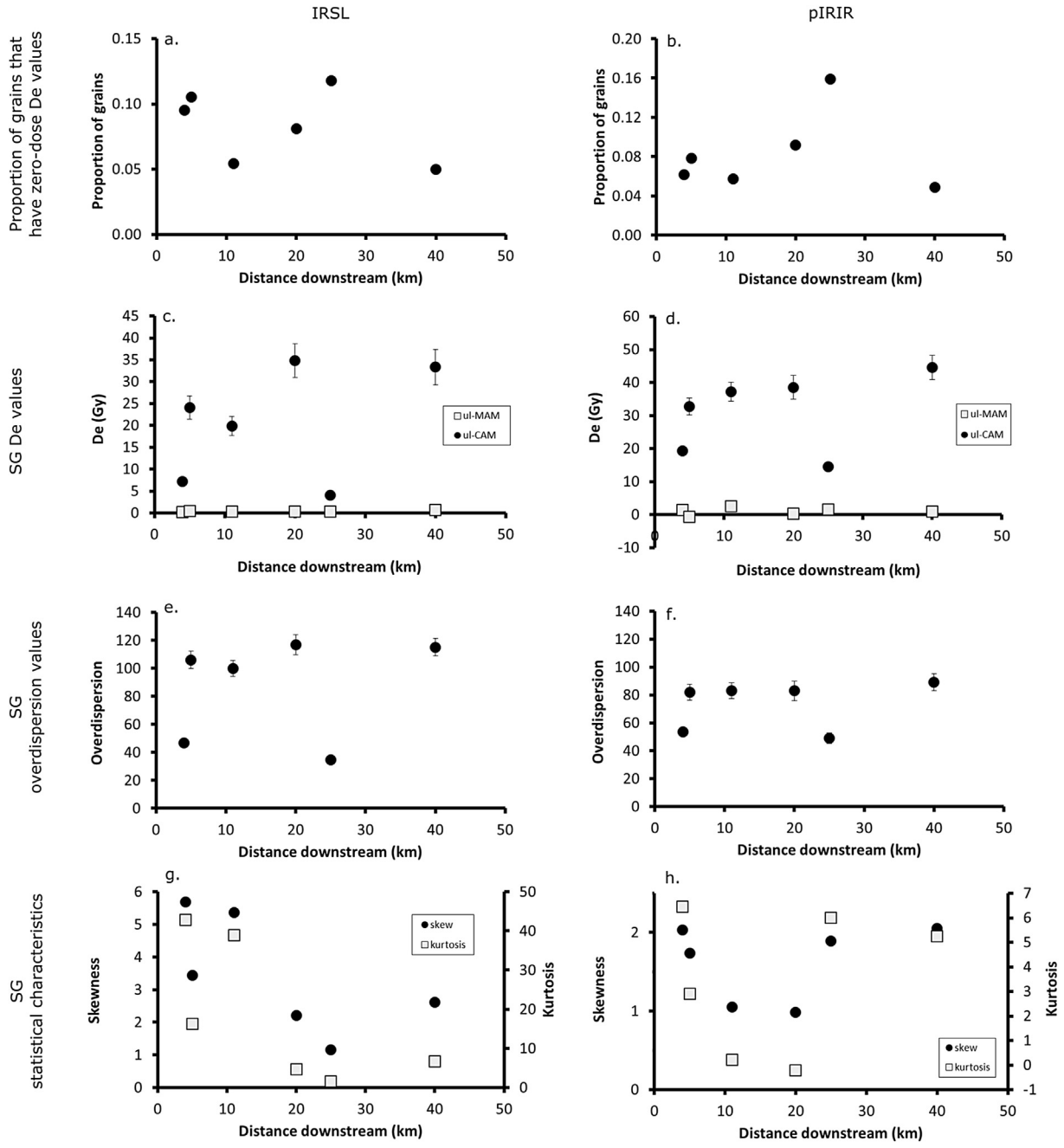

Fig. 7. SG IRSL and pIRIR data for K-feldspar samples from the Pitze River showing (a and b) the proportion of grains that yield modern age D_e values, (c and d) the SG D_e values, (e and f) the SG overdispersion values, and (g and h) the skewness and kurtosis of SG D_e distributions.

slowly or remaining consistent, while the pIRIR signal increases linearly throughout (Fig. 5a). This difference between (i) the laboratory and natural signals and (ii) the natural IRSL and the natural pIRIR signals is not currently understood, but the latter could possibly result from the contribution of differently-sensitised sediments from side catchments to the bedload. Further investigations of the K-feldspar laboratory and natural behaviour warrant further research.

5.4. Skewness and kurtosis

In addition to sensitivity and bleaching, the skewness and kurtosis of the SG quartz D_e datasets from Wollombi Brook increase with transport distance (Fig. 3h). With the exception of the most downstream sample (WB7) this pattern is not the result of high-De outliers; the skewness and kurtosis of all other samples continue to increase with transport distance after the sequential removal of the highest D_e values. The pattern of increasing skewness and kurtosis downstream follows the same pattern of increasing bleachability, as shown through the number of well bleached grains (Fig. 3b) and the increasingly accurate CAM (MGA), MAM (MGA), and ul-CAM (SG) age estimates. The observation that the better-bleached samples from Wollombi also have the most highly skewed D_e datasets directly contradicts previously reported observations that high skewness is indicative of incomplete bleaching (e.g., Olley et al., 1999; Bailey and Arnold, 2006; Summa-Nelson and Rittenour,

Table 6
SG IRSL and pIRIR data for K-feldspar samples from the Pitze River.

Signal	Sample name	n = measured/accepted	Skew	Kurtosis	modern grains (%)	OD (%)	ul-CAM D_e (Gy)	ul-MAM D_e (Gy)
IRSL								
	PT1	300/263	5.7	42.8	10	47 ± 2	7.20 ± 0.33	0.23 ± 0.15
	PT2	200/171	3.4	16.3	11	106 ± 6	24.11 ± 2.69	0.50 ± 0.10
	PT3	200/166	5.4	38.8	5	100 ± 6	19.90 ± 2.15	0.31 ± 0.11
	PT5	200/148	2.2	4.6	8	117 ± 7	34.83 ± 3.86	0.38 ± 0.10
	PT6	200/161	1.2	1.6	12	35 ± 3	4.03 ± 0.25	0.32 ± 0.08
	PT8	200/180	2.6	6.7	5	115 ± 6	33.34 ± 4.03	0.76 ± 0.08
pIRIR								
	PT1	300/195	2.0	6.4	6	54 ± 3	19.26 ± 0.94	1.38 ± 0.63
	PT2	200/128	1.7	2.9	8	82 ± 6	32.69 ± 2.55	−0.63 ± 0.97
	PT3	200/122	1.1	0.2	6	83 ± 6	37.30 ± 2.89	2.58 ± 1.14
	PT5	200/87	1.0	−0.2	9	83 ± 7	38.55 ± 3.63	0.25 ± 0.40
	PT6	200/126	1.9	6.0	16	49 ± 4	14.56 ± 0.90	1.52 ± 0.74
	PT8	200/123	2.1	5.2	5	89 ± 6	44.52 ± 3.68	0.89 ± 1.71

2012), and suggests that the skewness of a D_e dataset may not be an appropriate indicator for bleaching. This conclusion is supported by the SG D_e data from the Cooper Creek and Pitze River, which exhibit no relationship between skewness or kurtosis with the proportion of zero-dose grains, CAM (SG and MGA), MAM (MGA).

6. Conclusions

In this study we observed varying patterns in the quartz OSL and K-feldspar IRSL and pIRIR sensitivities, bleaching, and SG D_e distributions with the distance downstream for modern age bedload samples from three distinct rivers. The quartz OSL and K-feldspar IRSL and pIRIR signals increase with downstream transport distance in two rivers, thus corroborating previous observations for quartz (Pietsch et al., 2008; Sawakuchi et al., 2011) and showing that IRSL signals from K-feldspar also increase in response to reworking cycles. Increasing transport distance also results in better bleaching of the OSL signal from quartz samples due to more grains being exposed to sunlight. All bedload samples contain many well bleached quartz grains, and while the use of the MAM on MGA data yields small overestimates, the SG MAM results consistently yielded the best estimates of burial dose for all samples. Skewness and kurtosis estimates show no consistent relationship with bleaching (residual or proportion of zero-dose grains) for Cooper Creek or Pitze River SG D_e datasets. By contrast these statistical measures increase consistently with downstream transport distance for SG data from Wollombi Brook samples. These results question the applicability of the skewness-value of a D_e dataset as an accurate indicator for bleaching. Finally, K-feldspar grains yielded residual MAM D_e values as high as 59 Gy and 81 Gy for the IRSL and pIRIR signals, respectively. However, SG measurements show that the IRSL and pIRIR signals from 5 to 15% of K-feldspar grains in each samples yield zero-dose D_e values. The MAM can be used to identify these well bleached K-feldspar grains in SG D_e datasets with low fading rates and accurate burial doses can be estimated, thus providing a valuable tool for future fluvial research in regions where poor OSL characteristics prevent the use of quartz as a dosimeter.

Acknowledgements

This study was performed during the course of an Australian Research Council Discovery Project (DP1096911 to TJC) and an Austrian Science Fund project (FWF grant 24924–G19 to MCM). We are grateful to John Jansen, Toshiyuki Fujioka, and Jan-Hendrik May for their help in collecting samples from Cooper Creek and discussing the study. Kornelia Pellegrini is thanked for her assistance in the laboratory. Two anonymous reviewers are thanked for helping to improve this manuscript.

Appendix A. Supplementary data

Supplementary data related to this article can be found at http://dx.doi.org/10.1016/j.quageo.2017.06.005.

References

Aitken, M.J., 1998. An Introduction to Optical Dating: the Dating of Quaternary Sediments by the Use of Photon-stimulated Luminescence. Oxford University Press, Oxford.
Alexanderson, H., 2007. Residual OSL signals from modern Greenlandic river sediments. Geochronometria 26 (1), 1–9. http://doi.org/10.2478/v10003-007-0001-6.
Alexanderson, H., Murray, A.S., 2012. Luminescence signals from modern sediments in a glaciated bay, NW Svalbard. Quat. Geochronol. 10, 250–256. http://doi.org/10.1016/j.quageo.2012.01.001.
Arnold, L.J., Roberts, R.G., 2009. Stochastic modelling of multi-grain equivalent dose (De) distributions: implications for OSL dating of sediment mixtures. Quat. Geochronol. 4 (3), 204–230. http://doi.org/10.1016/j.quageo.2008.12.001.
Arnold, L.J., Roberts, R.G., Galbraith, R.F., DeLong, S.B., 2009. A revised burial dose estimation procedure for optical dating of young and modern-age sediments. Quat. Geochronol. 4 (4), 306–325. http://doi.org/10.1016/j.quageo.2009.02.017.
Auclair, M., Lamothe, M., Huot, S., 2003. Measurement of anomalous fading for feldspar IRSL using SAR. Radiat. Meas. 37 (4–5), 487–492. http://doi.org/10.1016/S1350-4487(03)00018-0.
Bailey, R.M., Arnold, L.J., 2006. Statistical modelling of single grain quartz De distributions and an assessment of procedures for estimating burial dose. Quat. Sci. Rev. 25 (19–20), 2475–2502. http://doi.org/10.1016/j.quascirev.2005.09.012.
Bøtter-Jensen, L., Andersen, C.E., Duller, G.A.T., Murray, A.S., 2003. Developments in radiation, stimulation and observation facilities in luminescence measurements. Radiat. Meas. 37, 535–541.
Colarossi, D., Duller, G.A.T., Roberts, H.M., Tooth, S., Lyons, R., 2015. Comparison of paired quartz OSL and feldspar post-IR IRSL dose distributions in poorly bleached fluvial sediments from South Africa. Quat. Geochronol. 30, 233–238. http://doi.org/10.1016/j.quageo.2015.02.015.
Duller, G.A.T., 2003. Distinguishing quartz and feldspar in single grain luminescence measurements. Radiat. Meas. 37 (2), 161–165. http://doi.org/10.1016/S1350-4487(02)00170-1.
Durcan, J.A., Duller, G.A.T., 2011. The fast ratio: a rapid measure for testing the dominance of the fast component in the initial OSL signal from quartz. Radiat. Meas. 46 (10), 1065–1072. http://doi.org/10.1016/j.radmeas.2011.07.016.
Erskine, W.D., Melville, M.D., 2008. Geomorphic and stratigraphic complexity: Holocene alluvial history of upper Wollombi Brook, Australia. Geogr. Ann. Ser. A, Phys. Geogr. 90, 19–35.
Fiebig, M., Preusser, F., 2007. Investigating the amount of zeroing in modern sediments of River Danube, Austria. Quat. Geochronol. 2 (1–4), 143–149. http://doi.org/10.1016/j.quageo.2006.09.001.
Fuchs, M.C., Böhlert, R., Krbetschek, M., Preusser, F., Egli, M., 2013. Exploring the potential of luminescence methods for dating Alpine rock glaciers. Quat. Geochronol. 18, 17–33. http://doi.org/10.1016/j.quageo.2013.07.001.
Galbraith, R.F., Roberts, R.G., Laslett, G.M., Yoshida, H., Olley, J.M., 1999. Optical dating of single and multiple grains of quartz from Jinmium rock shelter, northern Australia: part I, experimental design and statistical models. Archaeometry 41, 339–364.
Gliganic, L.A., Cohen, T.J., Slack, M., Feathers, J.K., 2016. Sediment mixing in aeolian sandsheets identified and quantified using single-grain optically stimulated

luminescence. Quat. Geochronol. 32, 53–66. http://doi.org/10.1016/j.quageo.2015.12.006.
Godfrey-Smith, D.I., Huntley, D.J., Chen, W.H., 1988. Optical dating studies of quartz and feldspar sediment extracts. Quat. Sci. Rev. 7 (3–4), 373–380. http://doi.org/10.1016/0277-3791(88)90032-7.
Gray, H.J., Mahan, S.A., 2015. Variables and potential models for the bleaching of luminescence signals in fluvial environments. Quat. Int. 362, 42–49. http://doi.org/10.1016/j.quaint.2014.11.007.
Habeck-Fardy, A., Nanson, G.C., 2014. Environmental character and history of the Lake Eyre Basin, one seventh of the Australian continent. Earth-Science Rev. 132, 39–66. http://doi.org/10.1016/j.earscirev.2014.02.003.
Hu, G., Zhang, J.F., Qiu, W.L., Zhou, L.P., 2010. Residual OSL signals in modern fluvial sediments from the Yellow River (HuangHe) and the implications for dating young sediments. Quat. Geochronol. 5 (2–3), 187–193. http://doi.org/10.1016/j.quageo.2009.05.003.
Huntley, D.J., Lamothe, M., 2001. Ubiquity of anomalous fading in K-feldspars and the measurement and correction for it in optical dating. Can. J. Earth Sci. 38 (7), 1093–1106. http://doi.org/10.1139/e01-013.
Huntley, D.J., Godfrey-Smith, D.I., Thewalt, M.L.W., 1985. Optical dating of sediments. Nature 313, 105–107. http://doi.org/10.1038/313105a0.
Jain, M., Murray, A.S., Botter-Jensen, L., 2004. Optically stimulated luminescence dating: how significant is incomplete light exposure in fluvial environments? Quaternaire 15, 143–157.
Jansen, J.D., Nanson, G.C., Cohen, T.J., Fujioka, T., Fabel, D., Larsen, J.R., et al., 2013. Lowland river responses to intraplate tectonism and climate forcing quantified with luminescence and cosmogenic 10Be. Earth Planet. Sci. Lett. 366, 49–58. http://doi.org/10.1016/j.epsl.2013.02.007.
Kreutzer, S., Schmidt, C., Fuchs, M.C., Dietze, M., Fischer, M., Fuchs, M., 2012. Introducing an R package for luminescence dating analysis. Anc. TL 30 (1), 1–8.
Lawson, M.J., Roder, B.J., Stang, D.M., Rhodes, E.J., 2012. OSL and IRSL characteristics of quartz and feldspar from southern California, USA. Radiat. Meas. 47 (9), 830–836. http://doi.org/10.1016/j.radmeas.2012.03.025.
Lepper, K., Larsen, N.A., McKeever, S.W.S., 2000. Equivalent dose distribution analysis of Holocene eolian and fluvial quartz sands from Central Oklahoma. Radiat. Meas. 32 (5), 603–608. http://doi.org/10.1016/S1350-4487(00)00093-7.
Lowick, S.E., Trauerstein, M., Preusser, F., 2012. Testing the application of post IR-IRSL dating to fi ne grain waterlain sediments. Quat. Geochronol. 8, 33–40. http://doi.org/10.1016/j.quageo.2011.12.003.
McGuire, C., Rhodes, E.J., 2015. Determining fluvial sediment virtual velocity on the Mojave River using K-feldspar IRSL: initial assessment. Quat. Int. 362, 124–131. http://doi.org/10.1016/j.quaint.2014.07.055.
Mogessie, A., Purtscheller, F., Tessadri, R., 1985. Geochemistry of amphibolites from the Ötztal-stubai complex (northern Tyrol, Austria). Chem. Geol. 51, 103–113.
Mukul, M., Jaiswal, M., Singhvi, A.K., 2007. Timing of recent out-of-sequence active deformation in the frontal Himalayan wedg: insights from the Darjiling sub-Himalaya, India. Geology 35 (11), 999–1002. http://doi.org/10.1130/G23869A.1.
Murray, A.S., Wintle, A.G., 2000. Luminescence dating of quartz using an improved single- aliquot regenerative-dose protocol. Radiat. Meas. 32, 57–73.
Murray, A.S., Wintle, A.G., 2003. The single aliquot regenerative dose protocol: potential for improvements in reliability. Radiat. Meas. 37, 377–381. http://doi.org/10.1016/S1350-4487(03)00053-2.
Murray, A., Olley, J.M., Caitcheon, G., 1995. Measurement of equivalent doses in quartz from contemporary water-lain sediments using optically stimulated luminescence. Quat. Geochronol. 14, 365–371.
Nanson, G.C., Price, D.M., Jones, B.G., Maroulis, J.C., Coleman, M., Bowman, H., et al., 2008. Alluvial evidence for major climate and flow regime changes during the middle and late Quaternary in eastern central Australia. Geomorphology 101, 109–129. http://doi.org/10.1016/j.geomorph.2008.05.032.
Nian, X., Bailey, R.M., Zhou, L., 2012. Investigations of the post-IR IRSL protocol applied to single K-feldspar grains from fluvial sediment samples. Radiat. Meas. 47 (9), 703–709. http://doi.org/10.1016/j.radmeas.2012.03.024.
Olley, J.M., Caitcheon, G.G., Roberts, R.G., 1999. The origin of dose distributions in fuvial sediments, and the prospect of dating single grains from fuvial deposits using optically stimulated luminescence. Radiat. Meas. 30, 207–217.
Olley, J.M., Caitcheon, G., Murray, A., 1998. The distribution of apparent dose as determined by optically stimulated luminescence in small aliquots of fluvial quartz: implications for dating young sediments. Quat. Geochronol. 17, 1033–1040.
Pfiffner, A., 2009. Geologie der Alpen, first ed. Haupt Verlag.
Pietsch, T.J., Olley, J.M., Nanson, G.C., 2008. Fluvial transport as a natural luminescence sensitiser of quartz. Quat. Geochronol. 3 (4), 365–376. http://doi.org/10.1016/j.quageo.2007.12.005.
Preusser, F., Ramseyer, K., Schlüchter, C., 2006. Characterisation of low OSL intensity quartz from the New Zealand Alps. Radiat. Meas. 41 (7–8), 871–877. http://doi.org/10.1016/j.radmeas.2006.04.019.
Rasmus, P.L., Rose, D.M., Rose, G., 1969. Singleton 1:250000 Geological Sheet SI/56-01, first ed. Geological Survey of New South Wales, Sydney.
Rhodes, E.J., 2011. Optically stimulated luminescence dating of sediments over the past 200,000 years. Annu. Rev. Earth Planet. Sci. 39, 461–488. http://doi.org/10.1146/annurev-earth-040610-133425.
Rhodes, E.J., 2015. Dating sediments using potassium feldspar single-grain IRSL: initial methodological considerations. Quat. Int. 362, 14–22. http://doi.org/10.1016/j.quaint.2014.12.012.
Sawakuchi, A.O., Blair, M.W., DeWitt, R., Faleiros, F.M., Hyppolito, T., Guedes, C.C.F., 2011. Thermal history versus sedimentary history: OSL sensitivity of quartz grains extracted from rocks and sediments. Quat. Geochronol. 6 (2), 261–272. http://doi.org/10.1016/j.quageo.2010.11.002.
Sawakuchi, A.O., Guedes, C.C.F., Dewitt, R., Giannini, P.C.F., Blair Jr., M.W., D. R. N, Faleiros, F.M., 2012. Quartz OSL sensitivity as a proxy for storm activity on the southern Brazilian coast during the Late Holocene. Quat. Geochronol. 13, 92–102. http://doi.org/10.1016/j.quageo.2012.07.002.
Singarayer, J.S., Bailey, R.M., Ward, S., Stokes, S., 2005. Assessing the completeness of optical resetting of quartz OSL in the natural environment. Radiat. Meas. 40 (1), 13–25. http://doi.org/10.1016/j.radmeas.2005.02.005.
Spooner, N.A., 1994. The anomalous fading of infrared-stimulated luminescence from feldspars. Radiat. Meas. 23 (2–3), 625–632. http://doi.org/10.1016/1350-4487(94)90111-2.
Stokes, S., Bray, H.E., Blum, M.D., 2001. Optical resetting in large drainage basins: tests of zeroing assumptions using single-aliquot procedures. Quat. Sci. Rev. 20 (5–9), 879–885. http://doi.org/10.1016/S0277-3791(00)00045-7.
Summa-Nelson, M.C., Rittenour, T.M., 2012. Application of OSL dating to middle to late Holocene arroyo sediments in Kanab Creek, southern Utah, USA. Quat. Geochronol. 10, 167–174. http://doi.org/10.1016/j.quageo.2012.05.002.
Thomas, M.F., Nott, J., Murray, A.S., Price, D.M., 2007. Fluvial response to late Quaternary climate change in NE Queensland, Australia. Palaeogeogr. Palaeoclimatol. Palaeoecol. 251, 119–136. http://doi.org/10.1016/j.palaeo.2007.02.021.
Thomsen, K.J., Murray, A.S., Bøtter-Jensen, L., Kinahan, J., 2007. Determination of burial dose in incompletely bleached fluvial samples using single grains of quartz. Radiat. Meas. 42, 370–379. http://doi.org/10.1016/j.radmeas.2007.01.041.
Thomsen, K.J., Murray, A.S., Jain, M., Bøtter-Jensen, L., 2008. Laboratory fading rates of various luminescence signals from feldspar-rich sediment extracts. Radiat. Meas. 43 (9–10), 1474–1486. http://doi.org/10.1016/j.radmeas.2008.06.002.
Trauerstein, M., Lowick, S.E., Preusser, F., Schlunegger, F., 2014. Small aliquot and single grain IRSL and post-IR IRSL dating of fluvial and alluvial sediments from the Pativilca valley, Peru. Quat. Geochronol. 22, 163–174. http://doi.org/10.1016/j.quageo.2013.12.004.
Wintle, A.G., 1997. Luminescence dating: laboratory procedures and protocols. Radiat. Meas. 27 (5), 760–817.
Yoshida, H., Roberts, R.G., Olley, J.M., Laslett, G.M., Galbraith, R.F., 2000. Extending the age range of optical dating using single “supergrains” of quartz. Radiat. Meas. 32, 439–446.